Carborane Clusters

DOI: 10.1002/ange.201307333

Variable Photophysical Properties of Phosphorescent Iridium(III) Complexes Triggered by *closo*- and *nido*-Carborane Substitution**

Chao Shi, Huibin Sun, Xiao Tang, Wen Lv, Hong Yan, Qiang Zhao,* Jingxia Wang, and Wei Huang**

Dedicated to Professor Xiaozeng You on the occasion of his 80th birthday

Icosahedral *closo*-carboranes including 1,2-, 1,7-, and 1,12-$C_2B_{10}H_{12}$ (that is, *o*-, *m*-, and *p*-carborane) have been intensively investigated for decades owing to their unique 3D pseudo aromatic geometric structures and push–pull electronic properties.[1] Recently, more attention has been paid to optoelectronic properties of carborane-based materials.[2] However, the effects of carborane cage itself on photophysical properties of materials still need further investigation, especially for *o*-carborane derivatives, which possess an unusual C–C bond (in the range of 1.62–2.15 Å for the bond distance)[3] and usually quench luminescence.[2a–d] Better understanding of this phenomenon is important to guide further molecular design of carborane-containing luminescent materials. On the other hand, *nido*-carborane-functionalized luminescent compounds are less studied[4] in comparison to *closo*-carborane-based derivatives, despite hydrophilic *nido*-carborane derivatives being promising candidates for biological applications such as in bioimaging.

In the last decade, phosphorescent iridium(III) complexes have been widely used in organic light-emitting diodes (OLEDs),[5] chemosensors,[6] and bioimaging[7] owing to their stable chemical structure, high luminescent efficiency, and tunable excitation and emission wavelength over the whole visible range. However, few carborane-based phosphorescent iridium(III) complexes have been reported.[8] It is anticipated that introduction of carborane cages into phosphorescent iridium(III) complexes may further improve the photophysical properties of these complexes and allow better understanding the roles of carborane groups. As such, we chose the well-studied homoleptic triply cyclometalated phosphorescent iridium(III) complexes $[Ir(ppy)_3]$[9] (ppy = 2-phenylpyridine) as control compounds and synthesized a series of facial and meridional iridium(III) complexes containing *o*-, *m*-, or *p*-carboranyl units in the cyclometalated C^N ligand, denoted as *fac-o*, *fac-m*, and *fac-p* for facial complexes and *mer-o*, *mer-m*, and *mer-p* for meridional complexes (Scheme 1). The results demonstrate that introduction of *m*- and *p*-carborane cages can improve phosphorescence efficiency (Φ_P) of both facial and meridional structures. The luminescent efficiency of the *o*-carborane derivative *fac-o* exhibits solvent- or media-dependence, which is closely related to dielectric constant (ε) of media as the specific C–C bond of *o*-carborane is involved in excited state and highly sensible to media. A new phosphorescent iridium(III) complex containing *nido-o*-carborane cages has been prepared as well, which possesses stable chemical structure, excellent water solubility, high phosphorescence efficiency (absolute $\Phi_P = 0.36$ in aqueous solution), and a long emission lifetime, thus has been successfully applied in cellular bioimaging.

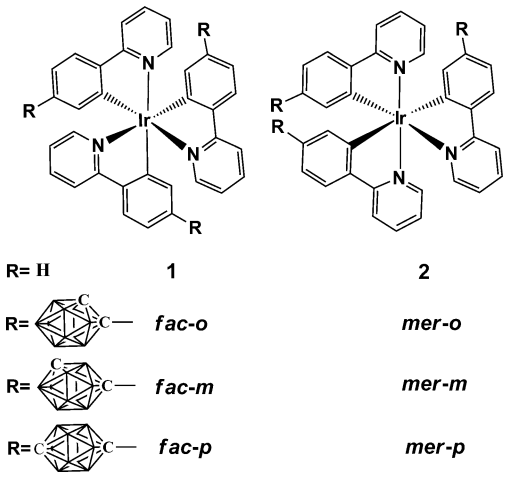

Scheme 1. The structures of *closo*-carborane-functionalized facial and meridional iridium(III) complexes.

All of the carborane-functionalized cyclometalated ligands (R-ppy) were prepared through an efficient Suzuki–Miyaura cross-coupling reaction[10] using 2-(6-phenyl-1,3,6,2-dioxazaborocan-2-yl)pyridine as a boron reagent (Supporting

[*] C. Shi, X. Tang, Prof. Dr. H. Yan
State Key Laboratory of Coordination Chemistry
School of Chemistry and Chemical Engineering, Nanjing University
Nanjing, Jiangsu 210093 (China)
E-mail: hyan1965@nju.edu.cn
H. Sun, W. Lv, Q. Zhao, J. Wang, W. Huang
Key Laboratory for Organic Electronics & Information Displays and Institute of Advanced Materials, Nanjing University of Posts and Telecommunications
Nanjing 210023 (P.R. China)
E-mail: iamqzhao@njupt.edu.cn
wei-huang@njupt.edu.cn

[**] The financial support from the National Natural Science Foundation of China (20925104, 21171098, 21271102), the Major State Basic Research Development Program of China (2013CB922100 and 2010CB923303), and high-performance computational center of Nanjing University is acknowledged.

Supporting information for this article is available on the WWW under http://dx.doi.org/10.1002/anie.201307333.

Information, Scheme S1) in yields of 80–85%. Three commonly used methods (A, B, and C in Scheme S1) were tried to synthesize the target iridium(III) complexes. Eventually, the target products were prepared by method A in yields of about 40% from the corresponding diketonate complexes $[(C^N)_2Ir(acac)]$ and C^N ligands. No products could be generated from the chloro-bridged dimer complexes $[\{(C^N)_2Ir(\mu\text{-}Cl)\}_2]$ and excess R-ppy ligands (method B). The method C by treating $[Ir(acac)_3]$ and free C^N ligands only led to yields of about 5%. Facial isomers are thermodynamically controlled products in comparison to dynamically controlled meridional isomers, similar to other reported iridium(III) analogues.[11] The new iridium(III) complexes were identified by ^1H, ^{13}C, ^{11}B NMR spectroscopy, MS, and single-crystal X-ray crystallography. The solid-state structures show that the facial isomer *fac-m* adopts a distorted octahedral coordination geometry with *cis* metalated carbon atoms, whereas the meridional isomer *mer-m* has two *trans* nitrogen atoms (Figure 1), similar to other reported iridium(III)

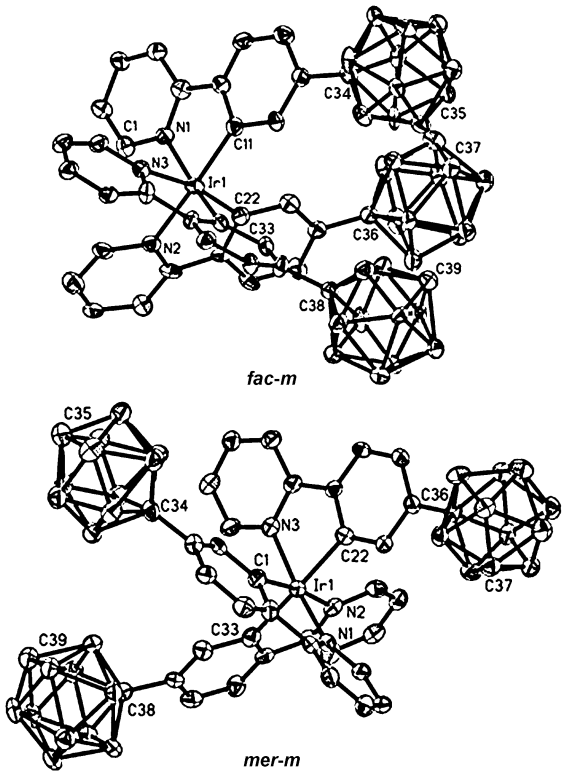

Figure 1. Crystal structures of *fac-m* and *mer-m*.[13]

complexes.[11] Note that all of the three carborane cages are oriented in the same direction in the facial structure, in contrast to only two in the meridional isomer. This leads to significant difference in molecular polarity, for example, the dipole moments (μ) of facial isomers are much larger than those of the meridional isomers on the basis of DFT calculations (Supporting Information, Figure S5 and Table S4). Additionally, the μ values of all the carborane-functionalized complexes are larger (that is, $\mu = 20.57$ for *fac-o* and $\mu = 12.22$ for *mer-o*) than those of the carborane-free complexes **1** ($\mu = 5.38$) and **2** ($\mu = 3.79$), indicating that carboranes can considerably increase polarity of molecules.

Spectroscopic studies show nearly no change in absorption spectra of both facial and meridional complexes in comparison to control complexes **1** and **2** (Supporting Information, Figure S1 and Table S2). Likewise, the emission spectra are almost the same except *mer*-o, which shows an approximate 20 nm blue shift versus complex **2** (Table 1; Supporting Information, Figure S2). The *m*- and *p*-carboranes

Table 1: Selected photophysical properties of Ir^{III} complexes.

Complex	PL[a,b] [nm]	Φ_p[a,b]	τ[a] [ns]	E_{onset}^{ox} [ev]	Eg[b] [ev]	HOMO/LUMO [ev][c]
fac-o	507	0.41	380	0.52	2.45	−5.32/−2.87
fac-m	507 (531)	0.46 (4.23%)	390	0.39	2.45	−5.19/−2.74
fac-p	507 (543)	0.48 (5.63%)	435	0.37	2.45	−5.17/−2.72
1	509 (534)	0.40 (3.23%)	340	0.25	2.44	−5.05/−2.61
mer-o	522	0.009	160	0.43	2.42	−5.23/−2.81
mer-m	543 (546)	0.051 (0.41%)	197	0.34	2.41	−5.14/−2.73
mer-p	545 (555)	0.053 (0.52%)	230	0.32	2.41	−5.12/−2.71
2	542 (567)	0.036 (0.32%)	187	0.14	2.41	−4.94/−2.51

[a] Recorded in degassed toluene solution at 298 K. [b] Data measured in solid state are given in parentheses. [c] HOMO [ev] $= -e(E_{onset}^{ox} + 4.8)$, $E_g = 1240/\lambda$, LUMO [ev] $= E_g +$ HOMO.

can increase luminescent efficiency of both types of structures to some extent in all of the solvents tested even though the Φ_P values of *mer-m* and *mer-p* are always very low, as determined by the meridional structure. The increase might be attributed to the large and rigid carborane cages that prevent rotation of molecules. Table 1 lists the Φ_P values of all complexes in toluene for comparison. However, *o*-carborane derivatives behave differently. For example, the luminescent efficiency of *fac-o* depends on solvents, such as $\Phi_P = 0.49$ in 1,4-dioxane, $\Phi_P = 0.35$ in diethyl ether, $\Phi_P = 0.15$ in $CHCl_3$, and $\Phi_P = 0$ in CH_2Cl_2 and methanol (Figure 2a and Table 2), despite no difference in emission wavelength with solvents. The phos-

Table 2: Photophysical properties of fac-o in different solvents.

Solvent	Dielectric constant[a]	Dipole moment[a] [D]	τ[b][ns]	Φ_p[b]
1,4-dioxane	2.25	0.45	500	0.49
benzene	2.27	0	468	0.46
toluene	2.38	0.36	380	0.41
Et_2O	4.30	1.15	160	0.35
$CHCl_3$	4.81	1.04	89	0.15
ethyl acetate	6.02	1.78	18	0.03
THF	7.50	1.75	–	0.01
CH_2Cl_2	9.10	1.60	–	–
CH_3OH	33.0	1.70	–	–
CH_3CN	37.5	3.92	–	–
DMF	38.0	3.82	–	–

[a] Data of the solvents. [b] Data in the degassed solvents at 298 K.

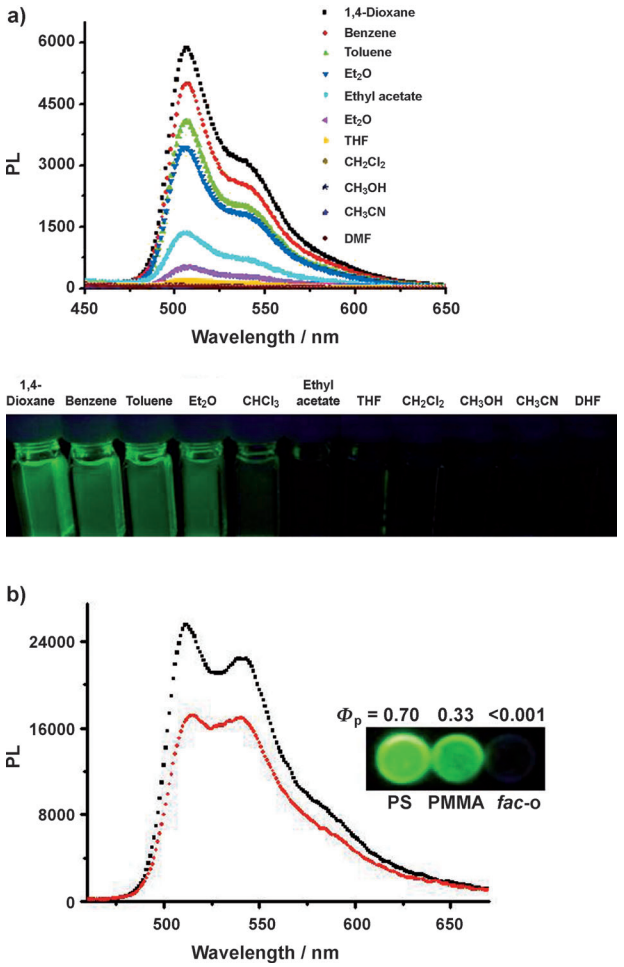

Figure 2. a) PL spectra of *fac-o* in eleven solvents with different dielectric constants at the same concentration (3×10^{-5} M). Bottom: corresponding luminescence photographs. b) PL spectra of *fac-o* in PS (2 wt%, black), PMMA (2 wt%, red), and a neat film (not visible). Inset: corresponding luminescence photographs.

phorescence efficiency and lifetime of *fac-o* in solution were observed to closely correlate to dielectric constants (ε) of solvents (Table 2). This phenomenon is also applicable to solid films (Figure 2b). For example, *fac-o* exhibits very strong emission in polystyrene film ($\varepsilon=2$, $\Phi_P=0.70$, 2 wt%) and weaker emission in PMMA film ($\varepsilon=4$, $\Phi_P=0.33$, 2 wt%), in sharp contrast to no emission in the neat film ($\Phi_P<0.001$); thus *fac-o* become strongly emissive by doping it in suitable host materials. These observed luminescence phenomena might be attributed to the special C–C bond of the *o*-carboranyl unit, which is sensitive to the outer environment. In the case of *mer-o*, the solvent effect is not evident, as luminescence is nearly quenched in all solvents tested. This is determined by the meridional structure, which feasibly leads to nonradiative decay.[11]

Electrochemical studies reveal that all complexes have reversible oxidation waves with potentials in the range of 0.14–0.52 eV (Supporting Information, Figure S4). The oxidation potentials of facial complexes are positively shifted relative to those of meridional analogues, demonstrating that the latter are more easily oxidized. The values of oxidation potentials follow the order of *fac-o* > *fac-m* > *fac-p* > **1** and *mer-o* > *mer-m* > *mer-p* > **2**, consistent with the order of electron-withdrawing ability of the carborane isomers. The results reflect that carborane isomers can increase oxidation potential and reduce the energy level of HOMO (Table 1), in agreement with our previous report.[8a]

To elucidate photophysical and electrochemical properties of these complexes, DFT calculations were performed to gain insight into structure–property relationships (Supporting Information, Figure S6–S10 and Tables S5–S7). In each case the lowest-energy absorption is mainly characterized by a HOMO→LUMO transition, which is the same as in the reported iridium(III) analogues.[11] The HOMO is located on the iridium(III) center and the phenyl ring of the cyclometalated ligand, but the LUMO is located on the pyridyl, phenyl, and partial carboranyl units, indicating that carboranes are involved in the excited states of all of the complexes. To explain why *fac-o* exhibits special photophysical properties that are dependent on solvents, structural optimizations were also conducted in benzene ($\varepsilon=2.27$), toluene ($\varepsilon=2.38$), diethyl ether ($\varepsilon=4.30$), CH_2Cl_2 ($\varepsilon=9.10$), methanol ($\varepsilon=33.0$), and acetonitrile ($\varepsilon=37.5$) with differing dielectric constants. The result showed that the distribution of electron cloud and energy levels of HOMO and LUMO are almost same in these solvents, thus the emission wavelength is independent on solvents. The frequency calculations with different solvents demonstrated that the vibration intensity of the C–C bond of *o*-carborane which is involved in excited state increases with the increased dielectric constant of solvent (Supporting Information, Figures S9, S10). However, the C–C vibration dissipates energy. Thus now it is easy to understand that *fac-o* exhibits strong emissions in solvents with low dielectric constants and weak or quenched emissions in solvents with high dielectric constants. Finally, the HOMO and LUMO energy levels descend owing to incorporation of carboranes, and follow the order of *fac-o* > *fac-m* > *fac-p* > **1** and *mer-o* > *mer-m* > *mer-p* > **2**, which is in agreement with the tendency as revealed by experimental data (Supporting Information, Figure S6 and S7).

In an attempt to explore potential applications of carborane-functionalized iridium(III) complexes, we synthesized a hydrophilic complex containing *nido-o*-carborane from *fac-o* in boiling ethanol in an isolated yield of 90%, denoted as *nido-fac-o* (Figure 3a). The ^{1}H NMR showed the characteristic broad B–H–B resonance of a *nido-o*-carborane. ^{11}B NMR showed less overlapping signals in a wider range for typical *nido-o*-carborane cage. The ESI-MS clearly demonstrated three peaks of $(M\text{-}K)^-$, $(M\text{-}2K)^{2-}$ and $(M\text{-}3K)^{3-}$. Its emission spectra in different solvents (Supporting Information, Figure S3) exhibited 10–40 nm red shifts in comparison to *fac-o*. To our delight, *nido-fac-o* has high phosphorescence efficiency (absolute $\Phi_P=0.36$) in aqueous solution, the highest among the reported water-soluble iridium(III) complexes.[12] In addition, *nido-fac-o* is also soluble in other polar solvents but shows differing phosphorescence efficiency, for example, absolute $\Phi_P=0.53$ in DMSO, absolute $\Phi_P=0.33$ in DMF and absolute $\Phi_P=0.06$ in CH_3OH. The maximum emission wavelength also shifts from 526 nm in CH_3OH to 543 nm in H_2O (Supporting Information,

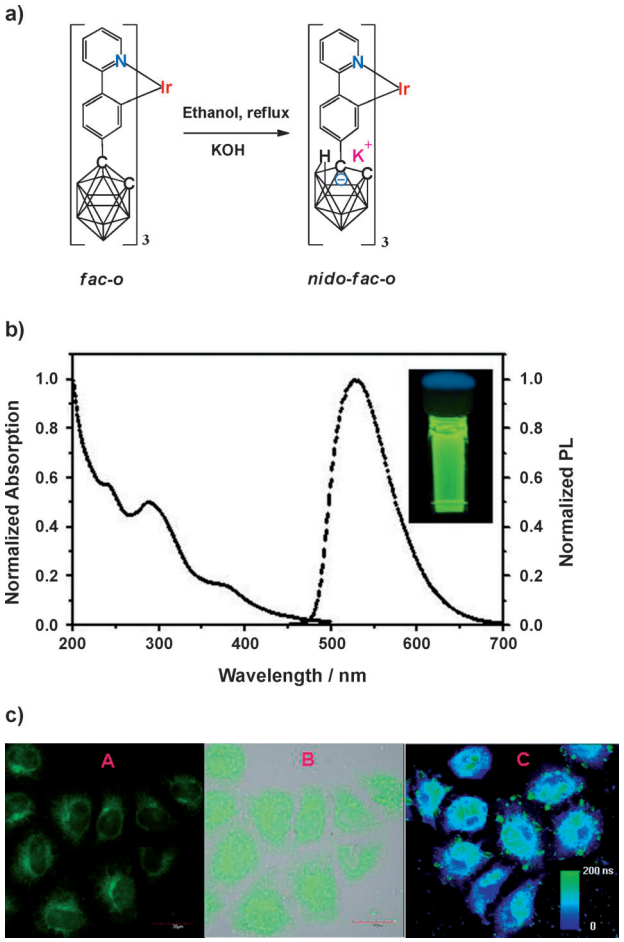

Figure 3. a) Synthesis of *nido-fac-o*. b) Absorption and PL spectra of *nido-fac-o* in aqueous solution (inset: luminescence photograph). c) Phosphorescent imaging (A), overlay images (B), and fluorescence lifetime imaging (C) of HeLa live cells incubated with *nido-fac-o* (10 μM) in phosphate buffered saline (PBS) for 60 min at 25 °C upon excitation at 405 nm.

Table S3), indicating that charge-transfer (CT) state has contributions to the excited states. DFT studies demonstrated that the LUMO of *nido-fac-o* is located on the pyridyl, phenyl, and partial carboranyl units (Supporting Information, Figure S11), which is the same as in *fac-o*. But the HOMO and HOMO−1 reside on the whole *nido-o*-carborane cage, the phenyl ring of the cyclometalated ligand and iridium(III) center (Supporting Information, Figure S11), which is obviously different from those in *fac-o*. The lowest triplet state (T_1) of *nido-fac-o* originates from HOMO→LUMO (0.29) and HOMO−1→LUMO (0.50) transitions (Supporting Information, Table S8). Thus, an intraligand charge transfer (ILCT) from *nido-o*-carborane to 2-phenylpyridine is involved in the excited states. This leads to distinctly different photophysical properties in contrast to *fac-o*.

Owing to the excellent solubility and high phosphorescence efficiency in aqueous solution, *nido-fac-o* was anticipated for potential applications in cellular imaging. Firstly, the cytotoxicity towards HeLa liver cancer cells was evaluated by MTT assay. After treatment of the cancer cells with different concentrations of *nido-fac-o* for 24 h, the cellular viabilities were estimated to be greater than 86% even at 100 μM, and no cytotoxicity was observed at 10 μM, which was utilized for imaging in this study (Supporting Information, Figure S12). Thus such low cytotoxicity is beneficial for prolonged live-cell imaging. The confocal laser scanning microscopic experiment showed bright intracellular luminescence, demonstrating that *nido-fac-o* was efficiently taken up by HeLa cells (Figure 3cA). Overlays of both brightfield image and confocal luminescence image confirmed that the luminescence was localized in the cytoplasm over nucleus and membrane (Figure 3cB), indicating that *nido-fac-o* was internalized into the cells rather than merely staining on the membrane surface. To utilize the long phosphorescence lifetime of *nido-fac-o* ($\tau = 1.0$ μs in aqueous solution), a fluorescence lifetime imaging (FLIM) experiment was conducted. As a result, high-quality long emission lifetime signal ($\tau = 168.0$ ns) was observed (Figure 3cC). This allows the phosphorescence signal to be recognized from short-lived fluorescence interference in a living system owing to their obviously different emission lifetimes. Thus the result has demonstrated the promising applications of *nido-fac-o* on the basis of its water solubility, high phosphorescence efficiency, and long emission lifetime.

In conclusion, *o*-, *m*-, and *p*-carboranes have been incorporated into homoleptic triply cyclometalated facial and meridional phosphorescent iridium(III) complexes. *m*- and *p*-Carboranes can improve luminescent efficiency of these complexes. In sharp contrast, the effect of *o*-carborane in the facial complex *fac-o* shows media dependence both in solution and solid state that conversely correlates to dielectric constant of media; thus *fac-o* shows strong emission in small dielectric constant media but quenched emission in large dielectric constant media. We found that quenching luminescence of *o*-carborane derivatives needs to meet two points: 1) *o*-carboranyl unit is involved in excited state; and 2) media has to be considered as the specific C−C bond in excited state is strongly affected by its outer surroundings. Furthermore, the water-soluble *nido-o*-carborane-functionalized iridium(III) complex (*nido-fac-o*) has been prepared, which has high phosphorescence efficiency and long emission lifetime in aqueous solution, thus has been successfully applied in bioimaging including fluorescence lifetime imaging. The preliminary results may direct further design of highly efficient carborane-functionalized phosphorescent metal complexes for optoelectronic and biological applications.

Received: August 20, 2013
Revised: September 15, 2013
Published online: October 16, 2013

Keywords: bioimaging · carboranes · iridium · phosphorescence

[1] a) A. M. Spokoyny, C. W. Machan, D. J. Clingerman, M. S. Rosen, M. J. Wiester, R. D. Kennedy, C. L. Stem, A. A. Sarieant, C. A. Mirkin, *Nat. Chem.* **2011**, *3*, 590; b) R. E. Williams, *Chem. Rev.* **1992**, *92*, 117; c) R. N. Grimes in *Carboranes, 2nd* ed., *Vol. 9*, Academic Press, New York, **2011**, pp. 301 – 540.

[2] a) K. Kokado, Y. Chujo, *Macromolecules* **2009**, *42*, 1418; b) K. Kokado, Y. Tokoro, Y. Chujo, *Macromolecules* **2009**, *42*, 2925;

c) K. Kokado, Y. Tokoro, Y. Chujo, *Macromolecules* **2009**, *42*, 9238; d) J. J. Peterson, M. Werre, Y. C. Simon, E. B. Coughlin, K. R. Carter, *Macromolecules* **2009**, *42*, 8594; e) J. J. Peterson, Y. C. Simon, E. B. Coughlin, K. R. Carter, *Chem. Commun.* **2009**, 4950; f) B. P. Dash, R. Satapathy, E. R. Gaillard, J. A. Maguire, N. S. Hosmane, *J. Am. Chem. Soc.* **2010**, *132*, 6578; g) K. Kokado, Y. Chujo, *J. Org. Chem.* **2011**, *76*, 316; h) J. J. Peterson, A. R. Davis, M. Werre, E. B. Coughlin, K. R. Carter, *ACS Appl. Mater. Interfaces* **2011**, *3*, 1796; i) B. P. Dash, R. Satapathy, E. R. Gaillard, K. M. Norton, J. A. Maguire, N. Chug, N. S. Hosmane, *Inorg. Chem.* **2011**, *50*, 5485; j) K.-R. Wee, W.-S. Han, D. W. Cho, S. Kwon, C. Pac, S. O. Kang, *Angew. Chem.* **2012**, *124*, 2731; *Angew. Chem. Int. Ed.* **2012**, *51*, 2677; k) K.-R. Wee, Y.-J. Cho, S. Jeong, S. Kwon, J.-D. Lee, I.-H. Suh, S. O. Kang, *J. Am. Chem. Soc.* **2012**, *134*, 17982; l) Y. Morisaki, M. Tominaga, Y. Chujo, *Chem. Eur. J.* **2012**, *18*, 11251; m) L. Weber, J. Kahlert, R. Brockhinke, L. Böhling, A. Brockhinke, H. G. Stammler, B. Neumann, R. A. Harder, M. A. Fox, *Chem. Eur. J.* **2012**, *18*, 8347; n) L. Weber, J. Kahlert, L. Böhling, A. Brockhinke, H. G. Stammler, B. Neumann, R. A. Harder, M. A. Fox, *Dalton Trans.* **2013**, *42*, 2266; o) A. Harriman, M. A. H. Alamiry, J. P. Hagon, D. Hablot, R. Ziessel, *Angew. Chem.* **2013**, *125*, 6743; *Angew. Chem. Int. Ed.* **2013**, *52*, 6611.

[3] a) I. V. Glukhov, M. Y. Antipin, K. A. Lyssenko, *Eur. J. Inorg. Chem.* **2004**, 1379; b) B. W. Hutton, F. MacIntosh, D. Ellis, F. Herisse, S. A. Macgregor, D. McKay, V. P. Armstrong, G. M. Rosair, D. S. Perekalin, H. Tricas, A. J. Welch, *Chem. Commun.* **2008**, 5345; c) J. Llop, C. Viñas, F. Teixidor, L. Victor, R. Kivekas, R. Sillanpää, *Organometallics* **2001**, *20*, 4024; d) J. M. Oliva, N. L. Allan, P. von R. Schleyer, C. Viñas, F. Teixidor, *J. Am. Chem. Soc.* **2005**, *127*, 13538; e) R. Kivekas, R. Sillanpää, F. Teixidor, C. Viñas, R. Núñez, *Acta Crystallogr. C* **1994**, *50*, 2027; f) J. Llop, C. Viñas, J. Oliva, F. Teixidor, M. Flores, R. Kivekas, R. Sillanpää, *J. Organomet. Chem.* **2002**, *657*, 232; g) I. V. Glukhov, K. A. Lyssenko, A. A. Korlyukov, M. Y. Antipin, *Faraday Discuss.* **2007**, *135*, 203.

[4] a) O. Crespo, M. C. Gimeno, P. G. Jones, A. Laguna, J. M. López-de-Luzuriaga, M. Monge, J. L. Pérez, M. A. Ramón, *Inorg. Chem.* **2003**, *42*, 2061; b) F. Lerouge, C. Viñas, F. Teixidor, R. Núñez, A. Abreu, E. Xochitiotzi, R. Santillan, N. Farfán, *Dalton Trans.* **2007**, 1898; c) F. Lerouge, A. F. Ugalde, C. Viñas, F. Teixidor, R. Sillanpää, A. Abreu, E. Xochitiotzi, N. Farfán, R. Santillan, R. Núñez, *Dalton Trans.* **2011**, *40*, 7541; d) R. Visbal, I. Ospino, J. M. López-de-Luzuriaga, A. Laguna, M. C. Gimeno, *J. Am. Chem. Soc.* **2013**, *135*, 4712.

[5] a) M. A. Baldo, M. E. Thompson, S. R. Forrest, *Nature* **2000**, *403*, 750; b) S. Lamansky, P. Djurovich, D. Murphy, F. A. Razzaq, H. E. Lee, C. Adachi, P. E. Burrows, S. R. Forrest, M. E. Thompson, *J. Am. Chem. Soc.* **2001**, *123*, 4304; c) A. Tsuboyama, H. Iwawaki, M. Furugori, T. Mukaide, J. Kamatani, S. Igawa, T. Moriyama, S. Miura, T. Takiguchi, S. Okada, M. Hoshina, K. Ueno, *J. Am. Chem. Soc.* **2003**, *125*, 12971; d) A. M. Prokhorov, A. Santoro, J. A. G. Williams, D. W. Bruce, *Angew. Chem.* **2012**, *124*, 99; *Angew. Chem. Int. Ed.* **2012**, *51*, 95.

[6] a) Q. Zhao, F. Y. Li, C. H. Huang, *Chem. Soc. Rev.* **2010**, *39*, 3007; b) Y. You, Y. Han, Y. M. Lee, S. Y. Park, W. Nam, S. J. Lippard, *J. Am. Chem. Soc.* **2011**, *133*, 11488.

[7] a) D. L. Ma, W. L. Wong, W. H. Chung, F. Y. Chan, P. K. So, T. S. Lai, Z. Y. Zhou, Y. C. Leung, K. Y. Wong, *Angew. Chem.* **2008**, *120*, 3795; *Angew. Chem. Int. Ed.* **2008**, *47*, 3735; b) Q. Zhao, C. H. Huang, F. Y. Li, *Chem. Soc. Rev.* **2011**, *40*, 2508.

[8] a) C. Shi, H. B. Sun, Q. B. Jiang, Q. Zhao, J. X. Wang, W. Huang, H. Yan, *Chem. Commun.* **2013**, *49*, 4746; b) T. Kim, H. Kim, K. M. Lee, Y. S. Lee, M. H. Lee, *Inorg. Chem.* **2013**, *52*, 160.

[9] a) K. A. King, P. J. Spellane, R. J. Watts, *J. Am. Chem. Soc.* **1985**, *107*, 1431; b) M. A. Baldo, S. Lamansky, P. E. Burrows, M. E. Thompson, S. R. Forrest, *Appl. Phys. Lett.* **1999**, *75*, 4.

[10] a) P. B. Hodgson, F. H. Salingue, *Tetrahedron Lett.* **2004**, *45*, 685; b) C. Gutz, A. Lutzen, *Synthesis* **2010**, 85.

[11] A. B. Tamayo, B. D. Alleyne, P. I. Djurovich, S. Lamansky, I. Tsyba, N. N. Ho, R. Baa, M. E. Thompson, *J. Am. Chem. Soc.* **2003**, *125*, 7377.

[12] a) Y. Ma, S. J. Liu, H. R. Yang, Y. Q. Wu, C. J. Yang, X. M. Liu, Q. Zhao, H. Z. Wu, J. C. Liang, F. Y. Li, W. Huang, *J. Mater. Chem.* **2011**, *21*, 18974; b) Y. Ma, S. J. Liu, H. R. Yang, Y. Q. Wu, H. B. Sun, J. X. Wang, Q. Zhao, F. Y. Li, W. Huang, *J. Mater. Chem. B* **2013**, *1*, 319.

[13] CCDC 943587 (*fac-m*) and CCDC 943588 (*mer-m*) contain the supplementary crystallographic data for this paper. These data can be obtained free of charge from The Cambridge Crystallographic Data Centre via www.ccdc.cam.ac.uk/data_request/cif.